of low-volume samples. Our numerical calibration process enables once more to increase the accuracy of the CPM with an extracted value of 10.06 very close to the data given by the manufacturer with a unique calibration process.

4. CONCLUSION

In this study, we proposed a new calibration procedure applied to the cavity-perturbation technique based on a numerical interpolation allowing taking into account the geometrical and dielectric characteristics of the sample under study. This new calibration procedure enables to enlarge the validity of the CPM by taking into account the calibration dependency to the dielectric constant of the sample. As this technique appears to be very general, it could be applied to all types of resonant cavities. We plan to soon extend this technique to higher frequency bands and to other resonance modes.

REFERENCES

1. P. Queffelec, M. Le Floc'h, and P. Gelin, Broad band characterization of magnetic and dielectric thin film using a microstrip line, IEEE Instrum Meas 47 (1998), 956–963.
2. S. De Blasi, P. Queffelec, C. Prunier, W. Peng, and M. Guilloux-Viry, Broad band characterization in rectangular waveguide for microwave measurements of the permittivity of thin film ferroelectric layers, In: International Symposium on Integrated Ferroelectrics Digest, Bordeaux, France, 2007.
3. J. Sheen, Measurement of microwave dielectric properties by an amended cavity perturbation technique, Measurement 42 (2009).
4. J. Sheen, C.Y. Li, L.W. Ji, W.L. Mao, W. Liu, and C.A. Chen, Measurements of dielectric properties of TiO_2 thin films at microwave frequencies using an extended cavity perturbation technique, J Mater Sci Mater Eletron 21 (2010), 817–821.
5. M. Lin and M.N. Afsar, Measurement of dielectric and magnetic characteristics of Nickel Ferrite and Strontium Ferrite composite from 4.5 to 26.5 GHz frequency range, In: Instrumentation and Measurement Technical Conference Digest, Sorrento, Italy, 2006, pp. 836–838.
6. H. Lobato-Morales, A. Corona-Chavez, D.V.B. Murthy, and J.L. Olvera-Cervantes, Complex permittivity measurements using cavity perturbation technique with substrate integrated waveguide cavities, Rev Sci Instrum 81 (2010), 064704-1-064704-4.
7. L.F. Chen, C.K. Ong, C.P. Neo, V. V. Varadan, and V.K. Varadan, Microwave electronics: Measurement and material characterization, Wiley, Hoboken, NJ, 2004.
8. A.W. Kraszewski and S.O. Nelson, Observations on resonant cavity perturbation by dielectric objects, IEEE Trans Microwave Theory Tech 40 (1992), 151–155.
9. C.P.L. Rubinger and L.C. Costa, Building a resonant cavity for the measurement of microwave dielectric permittivity of high loss materials, Microwave Opt Technol Lett 49 (2007).
10. R.E. Collin, Foundations for microwave engineering, McGraw-Hill, New York, 1966, pp. 354–355.

EFFECTS OF EXCIMER LASER ANNEALING ON ELECTRICAL PROPERTIES OF ZNO POLYCRYSTALLINE FILMS DEPOSITED BY SPUTTERING

Gaoming Li, Jingwen Zhang, and Xun Hou
Department of Electronics Science and Technology, Xi'an Jiaotong University, No. 28, Xianning West Road, Xi'an, Shaanxi 710049, People's Republic of China; Corresponding author: jwzhang@mail.xjtu.edu.cn

Received 17 July 2013

ABSTRACT: *KrF excimer pulsed laser with wavelength of 248 nm was used to anneal the ZnO polycrystalline films deposited on silica glass substrates by radio frequency reactive sputtering. The laser pulse duration was 20 ns and energy density was 267 mJ/cm^2. After laser annealing, the resistance of the ZnO film measured by four-probe method decreased sharply. The resistance of samples under UV illumination at 254 nm decreased too. Moreover, the ratio of dark resistance to photoresistance reduced, this was not good for enhancing the sensitivity of the UV detector fabricated by the ZnO film. From the results of Hall Effect measurement, it was found that the carrier concentration of the samples increased and mobility of the samples decreased. The reason may be that melting and recrystallization induced by laser irradiation brought some defects into the films for large energy density.* © 2014 Wiley Periodicals, Inc. Microwave Opt Technol Lett 56:906–910, 2014; View this article online at wileyonlinelibrary.com. DOI 10.1002/mop.28233

Key words: *laser annealing; ZnO; electrical property; carrier concentration; carrier mobility*

1. INTRODUCTION

A lot of efforts have been put into the research of growing high-quality ZnO materials and optoelectronic devices fabrication based on ZnO. Because ZnO has some promising properties, such as wide bandgap (Eg = 3.37 eV) corresponding to the energy of photon in UV spectrum range, high binding energy of free exciton of 60 meV which is much higher than thermal energy of 26 meV at RT, fabrication process facility and no contamination to the environment [1–5].

To fabricate high-performance ZnO-based devices, such as light emitting diode, laser diodes, and photodetectors, ZnO thin films with high quality crystalline structure are needed. However, the ZnO films grown by sputtering and CVD method are always polycrystalline and have some native defects like oxygen vacancies (V_o) and interstitial Zinc (Zn_i) [1, 6–8]. So, annealing has been used to remove the defects and improve the crystalline quality.

Conventional annealing process is usually carried through a furnace. The temperature is so high that some flexible substrates and low melting point metal electrodes cannot withstand. So, the conventional thermal annealing technique is not compatible with some device fabrication processes. Then, a new annealing technique of rapid thermal annealing appears, in which the heating and cooling rate is very high so that the whole treatment does not take long. Its duration is just in the order of some minutes. A more effective annealing method by which a higher temperature can be reached in a much shorter time is laser annealing. It is worth noting that the laser density is a very important parameter to adjust for achieving satisfactory result. Some researchers have reported that the threshold laser density for ZnO is 150 mJ/cm^2 [9], laser pulses with density higher than which will cause crystalline structure deterioration. And, others believe the value is 450 mJ/cm^2 based on their experiments [10]. We found that some undesirable effects on the crystalline structure and electrical property will be engendered if the laser density is higher than 267 mJ/cm^2, which is much lower than 450 mJ/cm^2.

There are a lot of works on the melting model of the laser annealing process [11–13]. And, laser annealing effects on crystallinity and photoluminescence of ZnO films have been studied by many research groups [10, 14–16]. However, studies on electrical properties of laser annealed ZnO films deposited by sputtering have not been reported yet. In our work, we used UV

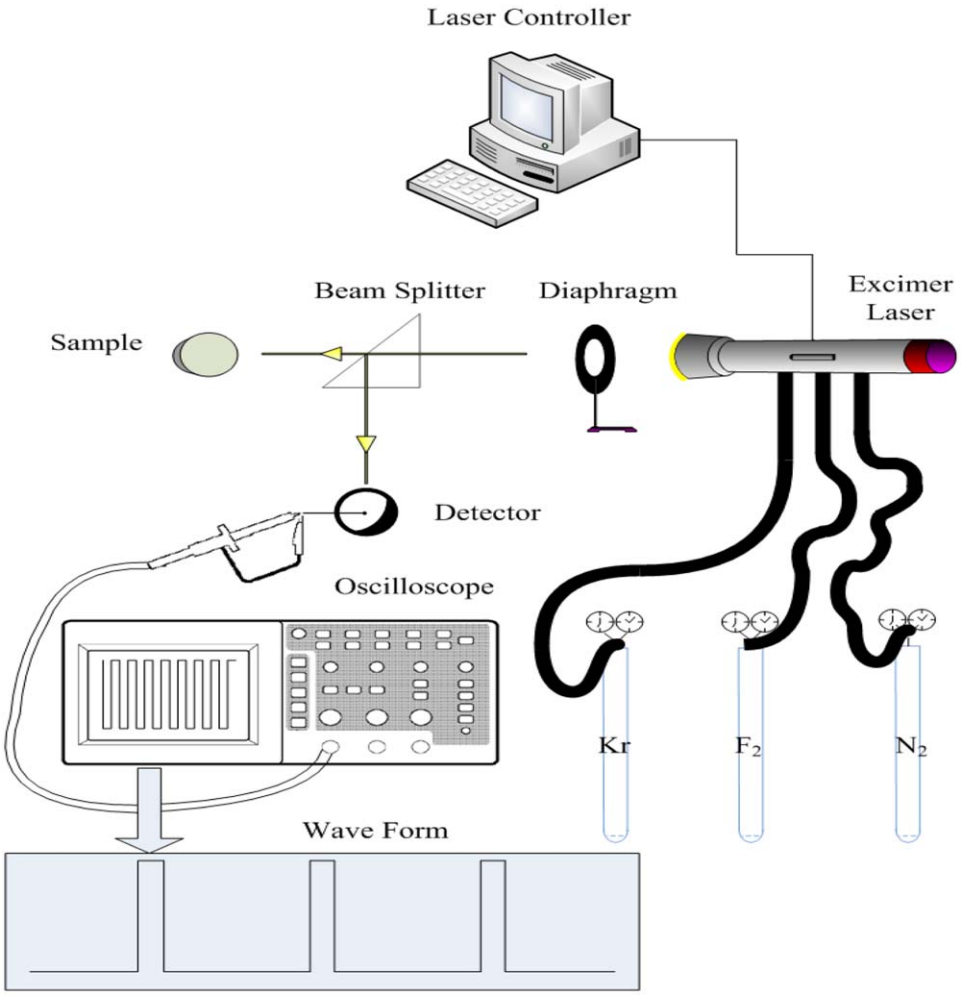

Figure 1 The schematic diagram of the experiment setup of laser annealing. [Color figure can be viewed in the online issue, which is available at wileyonlinelibrary.com]

KrF excimer pulsed laser to anneal the ZnO films fabricated by magnetron reactive sputtering. And, the influences of laser annealing on the electrical properties including resistance, carrier concentration, and carrier mobility of the ZnO films were studied.

2. METHODOLOGY

ZnO thin films were deposited by radio frequency (13.56 MHz) magnetron reactive sputtering. The sputtering target was ZnO ceramic wafer with purity of 99.99% and diameter of 50 mm. And, the 2-inch silica glass circular plates were used as substrates. Before sputtering, the substrates were rinsed, respectively, in acetone, ethanol, and deionized water, 10 min for each. The vacuum chamber in which sputtering took place was first evacuated until the pressure in it reached 5×10^{-4} Pa. Then, a mixture of gas composed of 35 sccm (standard cubic centimeters per minute) O_2 and 25 sccm Ar was flushed into the chamber. The pressure during the sputtering is 1.2 Pa and the substrate was heated at 400°C. Five samples were fabricated at different RF power, 150, 120, 90, 60, and 30 W corresponding to Sample A to Sample E, respectively. It took 90 min to finish the deposition of ZnO thin films.

KrF excimer pulsed laser was used to do the annealing. Its wavelength is 248 nm and the photon energy is 479.6 KJ/mol. The pulse duration is 20 ns. The spot size is rectangle with an area of 0.18 cm^2 and the energy of every laser pulse is 48 mJ. So, the laser density can be calculated, it is 267 mJ/cm^2. The repetition rate of the laser pulse is 1 Hz. Figure 1 shows the schematic diagram of the experiment setup. Sample A, B, and C

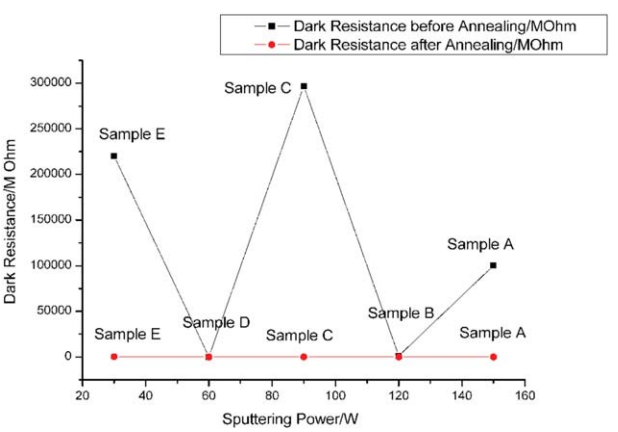

Figure 2 The dark resistance of each sample before and after annealing. [Color figure can be viewed in the online issue, which is available at wileyonlinelibrary.com]

TABLE 1 Resistance and Photoresistance Before and After Laser Annealing

	High Resistance Sample			Low Resistance Sample	
Sample	Sample A	Sample C	Sample E	Sample B	Sample D
Resistance before annealing	100.3 GΩ	296.8 GΩ	220.5 GΩ	1.13 GΩ	91 MΩ
Resistance after annealing	118 MΩ	50 MΩ	119 MΩ	37 MΩ	450 KΩ
Changing times	850	5936	1853	30.5	202
Photoresistance before annealing	128 MΩ	123 MΩ	119 MΩ	28 MΩ	17 MΩ
Photoresistance after annealing	25 MΩ	22 MΩ	40 MΩ	3.6 MΩ	250 KΩ
Changing times	5.1	5.6	3.0	7.8	68

were irradiated by laser pulse for 20 and 25 s for Sample D and E, namely, 20 laser pulses beat Sample A, B, and C's surface and 25 laser pulses beat Sample D and E's surface. Four-probe method was used to measure the samples resistance before and after laser annealing. The resistances of samples under UV illumination at 254 nm before and after annealing were also compared. Hall Effect measurement with van der Pauw configuration was used to measure the carrier concentration and mobility of the samples. The reason why laser annealing changed the carrier concentration and mobility was analyzed.

3. RESULTS AND DISCUSSION

We measured the resistance of the samples by Four-probe method. The dark resistance of each sample before and after laser annealing is shown in Figure 2 and Table 1. It can be seen that dark resistance of each sample decreases after laser processing, though the reducing extent of each sample is different, Sample A, C, and E exhibit a sharp fall of dark resistance after annealing as their dark resistance before annealing are so large. The resistances of these samples before laser processing are in the range of several hundred giga ohm. However, Sample B and D's dark resistance before annealing are not so large as others, and the change of dark resistance caused by laser pulse beating are not so violent either. As we know, dark resistance surely has relation with the crystalline structure of samples, even though the fully persuasive explanation of the dependence of crystalline structure on sputtering RF power has not been given. The experiment result may be interpreted like this: the high resistance samples have more orderly structure, which have fewer defects in the polycrystalline film than the low resistance samples. And so, the destructive effects of laser processing on polycrystalline structure of high resistance samples seem much severe than low resistance samples. Therefore, more defects which can generate more charge carriers are produced in the high resistance samples, then, the change of dark resistance of high resistance sample is larger. This interpretation can be demonstrated by carrier concentration provided by Hall Effect measurement.

The samples' photoresistance before and after laser annealing is shown in Figure 3 and Table 1. It is a well-known fact that ZnO film has a response to the UV illumination. In our experiment, we found that photoresistance of all samples decreases after laser processing. And, that is to say the photocurrent under a voltage bias will increase after annealing. This is very helpful to enhance the photoresponse of the UV detector which is fabricated by the as-annealed ZnO film. What is more, the changing trend of photoresistance is nearly the same as dark resistance. The samples with high photoresistance before laser pulse beating would decrease more than low photoresistance samples after laser processing. The photoresistances of Sample A, C, and E fall more substantially than those of Sample B and D. There is another point worth a particular attention, nearly all the samples' dark resistance after laser annealing is in the same range of the photoresistance of the samples before laser processing. It means that the charge carriers related to laser annealing induced defects have the same magnitude as photocarriers generated by UV light. Actually, this is not good for sensitive photodetector fabrication used the as-annealed ZnO film. Because the ratio of photo to dark current can be used to characterize the sensitivity of photodetector and it equals the reciprocal of the photo to dark resistance ratio.

The ratio of dark resistance to photoresistance of the film before and after laser annealing is shown in Figure 4. It is

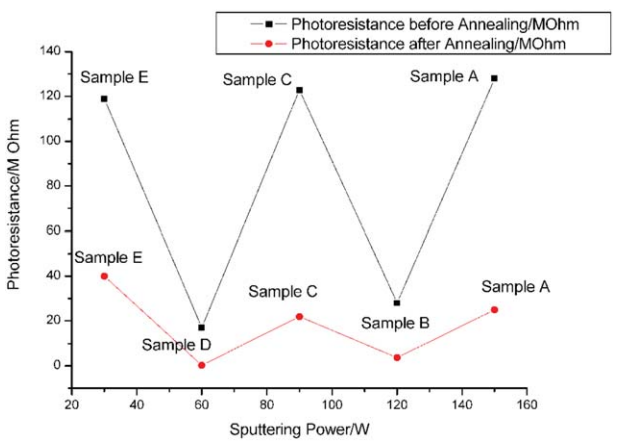

Figure 3 The photoresistance of each sample before and after annealing. [Color figure can be viewed in the online issue, which is available at wileyonlinelibrary.com]

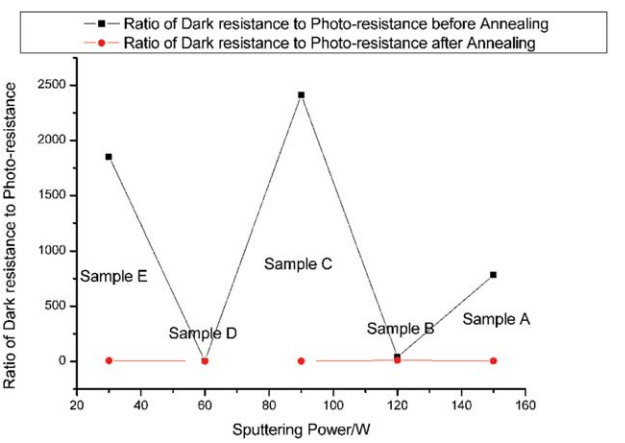

Figure 4 The ratio of dark resistance to photoresistance of the samples before and after laser annealing. [Color figure can be viewed in the online issue, which is available at wileyonlinelibrary.com]

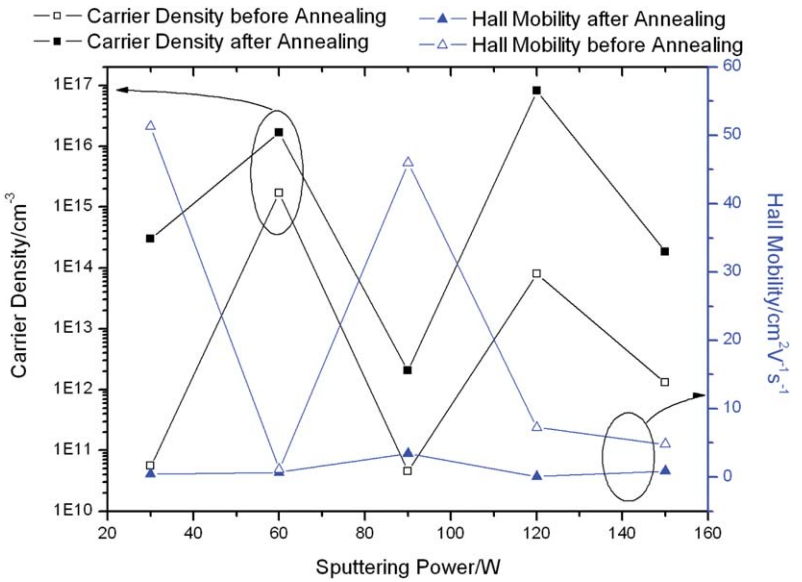

Figure 5 The carrier density and Hall mobility of the samples before and after laser processing. [Color figure can be viewed in the online issue, which is available at wileyonlinelibrary.com]

obvious that the figure of resistance ratio is very similar to the figure of dark resistance. It indicates that the influence of laser annealing on dark resistance plays an important role in electrical properties alternation caused by laser processing. And, it can be seen from Figure 3 that laser annealing makes the ratio of dark resistance to photoresistance decrease in different degrees, so does the ratio of photocurrent to dark current. It reduces the sensitivity of photodetector fabricated by the as-annealed films at the same time. From all the figures above, it can be found that the two groups of samples have nearly the same behavior, although they received different amount of laser pulses. One group consisted of Sample A, B, and C, including both high resistance sample and low resistance sample. The other group including high resistance Sample E and low resistance Sample D, has the nearly identical change with the previous group after laser pulse beating. So, it may be speculated that the number of laser pulses is not as important as laser density in laser annealing. That is reasonable as the characteristic time for laser induced heat diffusion through a thin film is of the order of 10^{-10} s, and the width of laser pulse is 20 ns which is much longer than the former time constant. There is enough time for heat diffusion so that there is no accumulative effect in the annealing process and the number of laser pulses influences little on the sample's electrical properties.

The change of carrier concentration and mobility after laser annealing reflects the variation of the crystalline structure of the samples after the interaction between laser pulses and sample's surface atom layer. Figure 5 shows the carrier density and Hall mobility of the samples before and after laser processing. It can be seen from Figure 5 that carrier density increases and Hall mobility decreases after laser pulses beating the samples. The reason for this change may be that crystalline structure especially in the layer near the surface has been demolished in some degree. And, a lot of defects which can play the role of donor or acceptor are produced in the interaction between sample's atom layer and laser pulses. Then, much more carriers generated after laser annealing. That is why the resistance went down after being treated by laser pulse. Hall mobility's decrease supports this interpretation for there may be more scattering by defects when charge carriers are transferred in the film. Actually, the density of laser pulse is just 267 mJ/cm^2 and it is much lower than the threshold density of 450 mJ/cm^2. But, crystalline structure deterioration still happened. We supposed that the threshold density is related to not only the type of material but also the crystallinity of the material, which has a close link with material fabrication condition. If the as-annealed film is used to fabricate photodetector, both dark current and photocurrent rise, however, the ratio of photocurrent to dark current falls. It is not good to enhance the sensitivity of the detector.

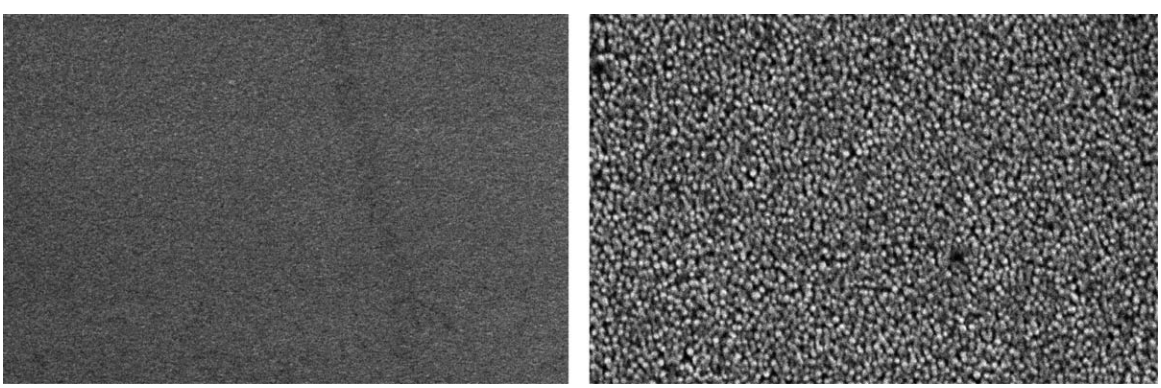

Figure 6 The SEM images of the samples before (left) and after (right) laser processing

The SEM images of Sample C before and after laser annealing is shown in Figure 6. We see that crystalline grains grow bigger after laser processing. The surface of the sample film becomes rough due to bigger grain size. The SEM images of other samples show the same change after annealing. That is an evidence of recrystallization during the interaction between laser pulses and sample surface atoms. It is also an equivalent effect to thermal annealing. Through Eq. (1), we can get the equivalent annealing temperature to the laser annealing.

$$c\rho\frac{\partial T}{\partial t}=I(z,t)\alpha+\frac{\partial}{\partial z}(k\frac{\partial T}{\partial z}) \quad (1)$$

In the Eq. (1), c, ρ, α, and k are the heat capacity, the mass density, the absorption coefficient, and the thermal conductivity, respectively. T and I are the temperature and light power density inside the sample film which are both functions of time t and depth z. According to the numerical method and parameters in the article of Baeri et al. [13], the equivalent temperature could reach 1135 K.

4. CONCLUSION

Polycrystalline ZnO films fabricated by radio frequency reactive sputtering with different sputtering power were annealed by KrF excimer pulsed laser. The resistances of the sample before and after laser processing were measured by Four-probe method. It is found that both dark resistance and photoresistance decrease after laser annealing. Moreover, the ratio of dark resistance to photoresistance decreases too. But, it is not advantageous to improve the sensitivity of the UV photodetector fabricated by the ZnO film. Hall Effect measurement was used to characterize the change of carrier concentration and Hall mobility after laser treatment. According to the experimental results, it is shown that carrier concentration increases but Hall mobility decreases after laser pulses beating the samples. It is believed that laser pulses beating the samples induces some defects when melting and recrystallization happens, though the density of laser pulse does not exceed the threshold density.

REFERENCES

1. U. Ozgur, Y.I. Alivov, C. Liu, A. Teke, M.A. Reshchikov, S. Doğan, V. Avrutin, S.-J. Cho, and H. Morkoç, A comprehensive review of ZnO materials and devices, J Appl Phys 98 (2005), 041301.
2. C. Yang, X.M. Li, Y.F. Gu, W.D. Yu, X.D. Gao, and Y.W. Zhang, ZnO based oxide system with continuous bandgap modulation from 3.7 to 4.9 eV, Appl Phys Lett 93 (2008), 112114.
3. Z. Bi, X. Yang, J. Zhang, X. Bian, D. Wang, X. Zhang, and X. Hou, A back-illuminated vertical-structure ultraviolet photodetector based on an RF-sputtered ZnO film, J Electron Mater 38 (2009), 609–612.
4. A. Yamamoto, T. Kido, T. Goto, Y. Chen, T. Yao, and A. Kasuya, Dynamics of photoexcited carriers in ZnO epitaxial thin films, Appl Phys Lett 75 (1999), 469–471.
5. H.S. Kang, J.S. Kang, J.W. Kim, and S.Y. Lee, Annealing effect on the property of ultraviolet and green emissions of ZnO thin films, J Appl Phys 95 (2004), 1246–1250.
6. D.C. Look, G.C. Farlow, P. Reunchan, S. Limpijumnong, S.B. Zhang, and K. Nordlund, Evidence for native-defect donors in n-type ZnO, Phys Rev Lett 95 (2005), 22502.
7. P.F. Carcia, R.S. McLean, M.H. Reilly, and G. Nunes, Transparent ZnO thin-film transistor fabricated by rf magnetron sputtering, Appl Phys Lett 82 (2003), 1117–1119.
8. Z.Z. Zhi, Y.C. Liu, B.S. Li, X.T. Zhang, Y.M. Lu, D.Z. Shen, and X.W. Fan, Effects of thermal annealing on ZnO films grown by plasma enhanced chemical vapour deposition from $Zn(C_2H_5)_2$ and CO_2 gas mixtures, J Phys D Appl Phys 36 (2003), 719–722.
9. T. Aoki, Y. Hatanaka, and D.C. Look, ZnO diode fabricated by excimer-laser doping, Appl Phys Lett 76 (2000), 3257–3258.
10. Y. Zhao and Y.J. Jiang, Effect of KrF excimer laser irradiation on the properties of ZnO thin films, J Appl Phys 103 (2008), 114903.
11. R.F. Wood and G.E. Giles, Macroscopic theory of pulsed-laser annealing. 1. Thermal transport and melting, Phys Rev B 23 (1981), 2923–2942.
12. P.M. Smith, P.G. Carey, and T.W. Sigmon, Excimer laser crystallization and doping of silicon films on plastic substrates, Appl Phys Lett 70 (1997), 342–344.
13. P. Baeri, S.U. Campisano, G. Foti, and E. Rimini, A melting model for pulsing-laser annealing of implanted semiconductors, J Appl Phys 50 (1979), 788–797.
14. I. Ozerov, M. Arab, V.I. Safarov, W. Marine, S. Giorgio, M. Sentis, and L. Nanai, Enhancement of exciton emission from ZnO nanocrystalline films by pulsed laser annealing, Appl Surf Sci 226 (2004), 242–248.
15. I. Ozerov, D. Nelson, A.V. Bulgakov, W. Marine, and M. Sentis, Synthesis and laser processing of ZnO nanocrystalline thin films, Appl Surf Sci 212 (2003), 349–352.
16. R.J. Winfield, L.H.K. Koh, S. O'Brien, and G.M. Crean, Excimer laser processing of ZnO thin films prepared by the sol-gel process, Appl Surf Sci 254 (2007), 855–858.

COMMON-MODE SUPPRESSED DIFFERENTIAL BANDPASS FILTER BASED ON OPEN COMPLEMENTARY SPLIT RING RESONATORS FABRICATED IN MICROSTRIP TECHNOLOGY WITHOUT GROUND PLANE ETCHING

Paris Vélez, Miguel Durán-Sindreu, Jordi Naqui, Jordi Bonache, and Ferran Martín
CIMITEC-Departament d'Enginyeria Electrònica, Universitat Autònoma de Barcelona, 08193 Bellaterra, Barcelona, Spain; Corresponding author: Email: Ferran.Martin@uab.es

Received 23 July 2013

ABSTRACT: *A differential (or balanced) bandpass filter based on open complementary split ring resonators (OCSRRs) coupled through admittance inverters is presented in this article. Pairs of OCSRRs are symmetrically placed in a mirror configuration between the strips of the differential line and are modeled by means of two series connected parallel resonators. For the differential (odd) mode, there is a virtual ground at the connecting plane between the OCSRR pairs, and the structure is roughly described by the canonical model of a bandpass filter, consisting of a cascade of shunt resonators coupled through admittance inverters. It is demonstrated that, through a proper design of the OCSRR stages, the common mode noise in the vicinity of the differential filter pass band can be efficiently suppressed. Due to the differential mode operation of the filter, it is not necessary to incorporate metallic vias to ground the OCSRRs. Moreover, as compared to other differential filters based on OCSRRs, defected ground structures are not present in the proposed filters. To illustrate the potential of the approach, two balanced bandpass filters are designed, fabricated, and characterized.* © 2014 Wiley Periodicals, Inc. Microwave Opt Technol Lett 56:910–916, 2014; View this article online at wileyonlinelibrary.com. DOI 10.1002/mop.28211

Key words: *split ring resonators; differential bandpass filters; microstrip technology*

1. INTRODUCTION

Split ring resonators (SRRs) [1] and their dual counterparts [complementary SRRs (CSRRs)] [2, 3] have been widely used